JOURNAL OF GEOPHYSICAL RESEARCH, VOL. 105, NO. D14, PAGES 17,895–17,910, JULY 27, 2000

Seasonal characteristics of tropospheric ozone production and mixing ratios over East Asia: A global three-dimensional chemical transport model analysis

Denise L. Mauzerall ,[1,2] Daiju Narita,[3] Hajime Akimoto,[3] Larry Horowitz,[4,2]
Stacy Walters,[5] Didier A. Hauglustaine,[6,2] and Guy Brasseur[7,2]

Abstract. We examine seasonal and geographical distributions of tropospheric ozone production and mixing ratios over East Asia with a global three-dimensional chemical transport model called Model of Ozone and Related Tracers, version 1 (MOZART 1). Net ozone production within the East Asian boundary layer exhibits three distinct seasonal cycles depending on region (north of 20°N, 5-20°N and south of 5°N). North of 20°N, net ozone production over East Asia from spring through autumn is found to have a maximum extending from 25°N-40°N and from central eastern China to Japan, resulting from the strong emission and transport of anthropogenic O_3 precursors. In winter, maximum O_3 production in this region occurs between 20°N and 30°N. This is a region of long-range transport. Over the Indochina peninsula, between 5°N and 20°N, net O_3 production is controlled by the seasonal cycle between wet and dry seasons and has a maximum at the end of the dry season due to emissions from biomass burning. South of 5°N, in the true tropics, O_3 mixing ratios are relatively constant throughout the year and do not exhibit a seasonal cycle. A spring-summer maximum of net O_3 production is found throughout the troposphere in East Asia. We estimate an annual net O_3 production in East Asia of 117 Tg/yr. Both model results and analysis of measurements of O_3/CO correlations over East Asia and Japan show strong variability as a function of both photochemical activity and seasonal meteorology, and indicate ozone export off the coast of East Asia in spring. An upper estimate of O_3 export from East Asia to the Pacific Ocean in the mid-1980s of 3.3 Gmol/d (58 Tg/yr) is obtained.

1. Introduction

East Asia is a region of the world with large and rapidly increasing anthropogenic emissions from combustion. Ozone is a secondary pollutant whose production in nonurban areas is primarily controlled by nitrogen oxide (NO_x) concentrations [*Liu et al.*, 1987] which are a primary product of combustion. *Benkovitz et al.* [1996] estimated that NO_x emissions from Asia (4.20 TgN/yr) were contributing 20% of the total global anthropogenic NO_x emissions for circa 1985. *Kato and Akimoto* [1992] estimated NO_x emissions in East Asia have increased by 58% from 1975 (2.05 TgN/yr) to 1987 (3.25 TgN/yr). Moreover, a projection of the future by *van Aardenne et al.* [1999] indicates that without the implementation of control measures, the emissions of NO_x from East Asia are expected to increase by 350% between 1990 and 2020.

Tropospheric O_3 has complex environmental effects. It is the primary precursor of the hydroxyl radical (OH) and thus plays a crucial role in controlling the oxidizing capacity of the atmosphere. O_3 absorbs infrared radiation and is a greenhouse gas in the upper troposphere [*Fishman et al.*, 1979; *Lacis et al.*, 1990; *Brasseur et al.*, 1998a]. At concentrations elevated above background levels O_3 damages natural vegetation [*Hogsett, et al.* 1997], reduces yields of agricultural crops [*Heck et al*, 1984], and is detrimental to human health [*Horvath and McKee*, 1994].

Recent research suggests that tropospheric ozone concentrations have increased in the lower troposphere over east Asia in recent decades and that the rate of increase is larger than in other areas of the northern midlatitudes [*Logan*, 1994; *Oltmans et al.*, 1998; *Lee et al.*, 1998]. Photochemical production of ozone in East Asia may increase ozone levels both within the region and downwind as Asian pollution has been observed to be transported over the Pacific Ocean [*Hoell et al.*, 1996] and to occasionally reach North America [*Jaffe et al.*, 1999; *Jacob et al.*, 1999; *Berntsen et al.*, 1999]. In addition, export of O_3 precursors (including NO_x and NO_x reservoir species) from East Asia is expected to enhance O_3 production downwind. A recent modeling study by *Jacob et al.* [1999] indicates that a tripling of Asian anthropogenic emissions from 1985 to 2010 is expected to increase monthly

[1]Woodrow Wilson School of Public and International Affairs, Princeton University, Princeton, New Jersey
[2]Formerly at the National Center for Atmospheric Research, Boulder, Colorado.
[3]Research Center for Advanced Science and Technology, University of Tokyo, Tokyo, Japan.
[4]Geophysical Fluid Dynamics Laboratory, Princeton, New Jersey
[5]National Center for Atmospheric Research, Boulder, Colorado.
[6]Service d'Aeronomie du CNRS, Université de Paris, Paris, France.
[7]Max Planck Institut für Meteorologie, Hamburg, Germany.

Paper number 2000JD900087.
0148-0227/00/2000JD900087$09.00

mean O_3 concentrations by 2-6 ppbv in the western United States, the maximum effect being in April-June.

The contribution of photochemical ozone production to regional budgets over the United States has been examined in several studies using three-dimensional (3-D) chemical tracer models (CTMs) [*McKeen et al.*, 1991; *Jacob et al.*, 1993; *Liang et al.*, 1998]. The continental-scale model analysis by *Jacob et al.* [1993] revealed that photochemical production of O_3 over the United States is substantial even on a hemispheric scale and may affect the global environment through its export out of this region. *Horowitz et al.* [1998] found that export of NO_x and organic nitrates from the U.S. continental boundary layer provided an important source of NO_x to the remote troposphere in the northern hemisphere where it is expected to contribute significantly to O_3 production. Few such budget analyses have been conducted for East Asia. Winter/spring and autumn budgets of the western Pacific have been examined using data from two aircraft flight campaigns Pacific Exploratory Mission–West A and B during September–October 1991 (PEM-West A) and February-March 1994 (PEM-West B) [*Liu et al.*, 1996; *Davis et al.*, 1996; *Crawford et al.*, 1997]. The impact of increased anthropogenic emissions in Asia on tropospheric O_3 over Asia in summer has been evaluated by *Berntsen et al.* [1996] using a global CTM. Using the Harvard global CTM, *Horowitz and Jacob* [1999] found that fossil fuel emissions from China have a large influence on NO_x concentrations over the Pacific Ocean. Describing the regional characteristics of ozone production, loss, and export from East Asia would therefore provide valuable insight into understanding the contribution of this rapidly developing part of the world on global O_3 budgets.

The purpose of this paper is to address regional and seasonal characteristics of photochemical ozone production and mixing ratios over East Asia. We examine seasonal geographical distributions of tropospheric ozone production and mixing ratios over this region with a global three-dimensional chemical transport model called Model of Ozone and Related Tracers, version 1 (MOZART 1) developed by *Brasseur et al.* [1998b] and evaluated by *Hauglustaine et al.* [1998a]. We also evaluate indirect evidence of export of ozone and its precursors from East Asia using correlations of O_3 and CO mixing ratios calculated in the model.

This paper is divided into five sections. We briefly describe the model and its evaluation in section 2. Geographical distributions of photochemical ozone production over East Asia and its seasonal variation and budgets are discussed in section 3. In section 4 we discuss horizontal variations in O_3/CO correlations and estimate the export of ozone and its precursors from East Asia. Conclusions are in section 5.

2. Model Description and Evaluation

MOZART 1 is a global three-dimensional chemical transport model which calculates the global distribution of 56 chemical species and the production and loss rates for O_3. A full description of MOZART 1 is given by *Brasseur et al.* [1998b]. A brief description is provided here. Horizontal resolution of MOZART 1 is approximately 2.8 ° in longitude and latitude (64 Gaussian grid cells in latitude and 128 equidistant in longitude), with 25 layers in the vertical between the Earth's surface and an upper boundary located at approximately 35 km altitude. The model includes surface emissions, photochemical conversions, advection, convection, and wet and dry deposition. Photochemical conversions include hydrocarbon chemistry and incorporate 112 chemical reactions and 28 photolysis reactions. Chemical and dynamical time steps are both 20 minutes. The model uses a global domain with surface boundary conditions specified by surface emissions and with the distribution of several long-lived species (O_3, NO_x, HNO_3, N_2O_5, CH_4, CO) prescribed above 60 mbar, according to monthly and zonally averaged values provided by the middle atmosphere 3-D Study of Transport and Chemical Reactions in the Stratosphere (STARS) model [*Brasseur et al.*, 1997]. Transport is driven with dynamical variables provided by the National Center for Atmospheric Research (NCAR) Community Climate Model (CCM2 library Ω0.5). The advection of chemical species uses the MATCH transport model developed by *Rasch et al.* [1997] which employs the semi-Lagrangian transport scheme of *Williamson and Rasch* [1989] and *Rasch and Williamson* [1990] and utilizes a mass conserving correction after each time step. Cloud formation and moist convective transport of chemical tracers are included and are taken from the convective parameterization of *Hack* [1994] as used in CCM2. No cloud chemistry is included. NO_x emissions from lightning are included and are assumed to produce 7 TgN/yr of reactive nitrogen which is distributed as a function of space and season according to the location of convective clouds in the CCM and following the parameterization of *Price and Rind* [1992].

Because industrial emissions from Asia are growing rapidly, the year which is represented by emission inventories will influence model results for eastern Asia. In MOZART 1 the surface emissions of biogenic and anthropogenic species are based on *Müller* [1992] with some adjustments to account for more recent data. *Müller* [1992] emission inventories are based on the Organization for Economic and Cooperative Development (OECD) emission estimates in 1980 for OECD countries (western Europe, North America, Japan, Australia, and New Zealand) and United Nations energy statistics in 1986 for non-OECD countries. NO_x emissions from fossil fuel combustion are taken from *Benkovitz et al.* [1996] for year 1985. MOZART 1 simulations thus use an anthropogenic emission scenario for East Asia approximately representing the mid-1980s. Since emissions are increasing rapidly in East Asia and we compare our model results with observations in Japan during 1996-1997, this may contribute to some discrepancies. The spatial and temporal distribution of biomass burned is taken from *Hao and Liu* [1994] in tropical regions and from *Müller* [1992] in nontropical regions.

MOZART 1 results have been evaluated by *Hauglustaine et al.* [1998a] with a variety of observations including NASA Global Tropospheric Experiment (GTE) aircraft flight campaign data, Climate Monitoring and Diagnostics Laboratory (CMDL) surface measurements of O_3, and vertical O_3 profiles from O_3 sondes. They showed that the model generally reproduces the observed mixing ratio of ozone and related species reasonably well with the exception of a general overprediction of nitric acid and a tendency to underpredict O_3 mixing ratios throughout the troposphere at mid to high latitudes.

While *Hauglustaine et al.* [1998] provide extensive comparisons of model results with data, their evaluation does not

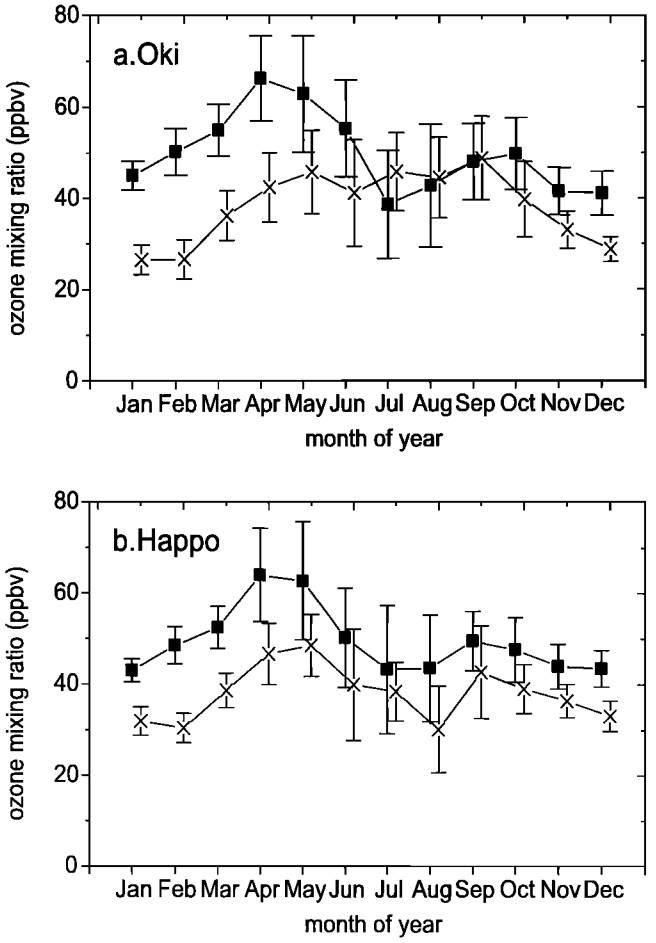

Figure 1. Seasonal variations of ozone mixing ratios from observations (1996-1997) and model results at (a) Oki (36°17'N, 133°11'E, 90 m asl) and (b) Happo (36°41'N, 137°48' E, 1840 m asl), Japan. Differences between the seasonal patterns at the two sites may be caused by the difference in altitude (1840 m and 90 m for Happo and Oki). Vertical bars on the observational data indicate one standard deviation calculated from hourly means. Vertical bars on the model results indicate one standard deviation in monthly averages calculated from daily 24-hour means.

include comparisons with surface measurements in East Asia, the region on which our study focuses. Thus we compare surface ozone and CO monitoring data measured at two remote sites in Japan (Oki and Happo) with model results. The Oki site is located on Dogo island 65 km from the Japanese mainland at latitude 36°17'N, longitude 133°11'E, and elevation 90 m above sea level (asl). The Happo site is situated in a mountainous region in central Japan (Japan Alps) at latitude, longitude, and altitude of 36°41'N, 137°48'E, and 1840 m asl. Since the model is intended to simulate a typical meteorological year rather than any given year, we focus on seasonal statistics in our comparisons. Monitoring data are obtained by averaging hourly data obtained during 1996-1997 using commercially available ultraviolet absorption (Dylec) and nondiffusive infrared absorption (Kimoto) instruments for O_3 and CO, respectively. Measurement details for each monitoring station are described by *Pochanart et al.* [1999].

Figure 1 shows the seasonal variation of O_3 at Oki (Figure 1a) and Happo (Figure 1b). The figure shows the model reproduces O_3 concentrations reasonably well in summer and autumn but underestimates O_3 mixing ratios in winter and spring at both Oki and Happo. Such under estimation by MOZART 1 in winter and spring is also observed at other measurement sites in East Asia (in Srinakarin and Inthanon, Thailand, and in Mondy, Russia, in Siberia (H. Akimoto, unpublished data, 1999), as well as other surface sites in the northern midlatitudes (Mace Head, Niwot Ridge, and Bermuda) [*Hauglustaine et al.*, 1998a]. This feature may be explained by a relatively low contribution of stratospheric O_3 to the troposphere in MOZART 1 due to the use of the semi-Lagrangian transport scheme and mass fixer. Since stratosphere to troposphere exchange is believed to maximize in winter at mid to high latitudes [*Holton*, 1990], low influx of stratospheric O_3 in MOZART 1 is likely to primarily depress winter tropospheric O_3 levels. In addition, since we are using climatological winds rather than assimilated winds representing 1996-1997, the winds may not accurately represent the conditions prevailing during the measurement period.

While the model underestimates the mixing ratio of O_3 in the winter/spring in East Asia, we found evidence that it

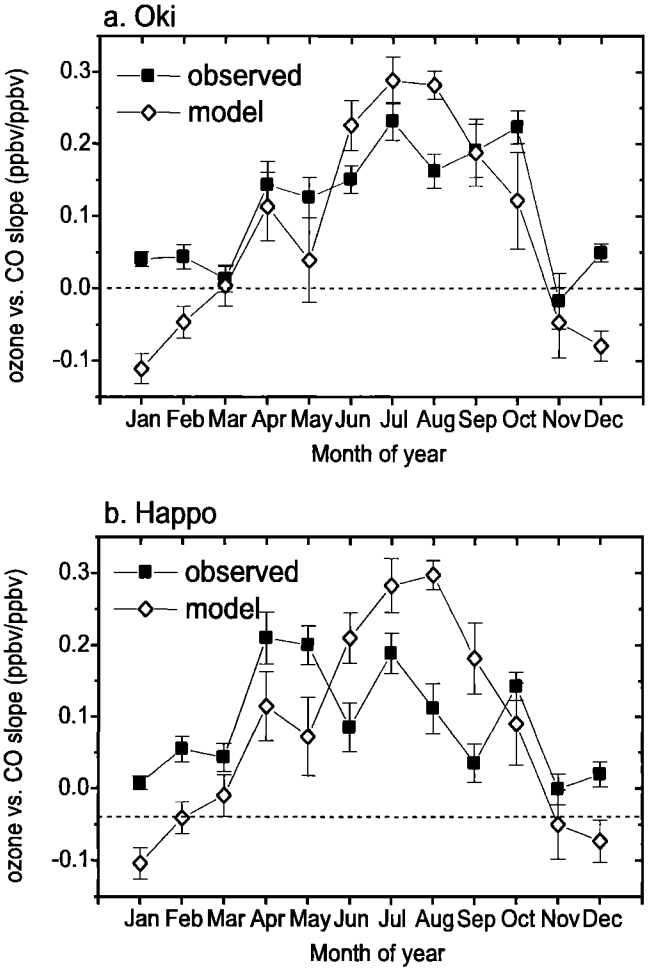

Figure 2. Seasonal variations of O_3/CO correlation slope obtained from observational and model data for (a) Oki and (b) Happo. Observational results are based on 1996-1997 data. One standard deviation in slope values for each month are indicated by vertical bars in the figures.

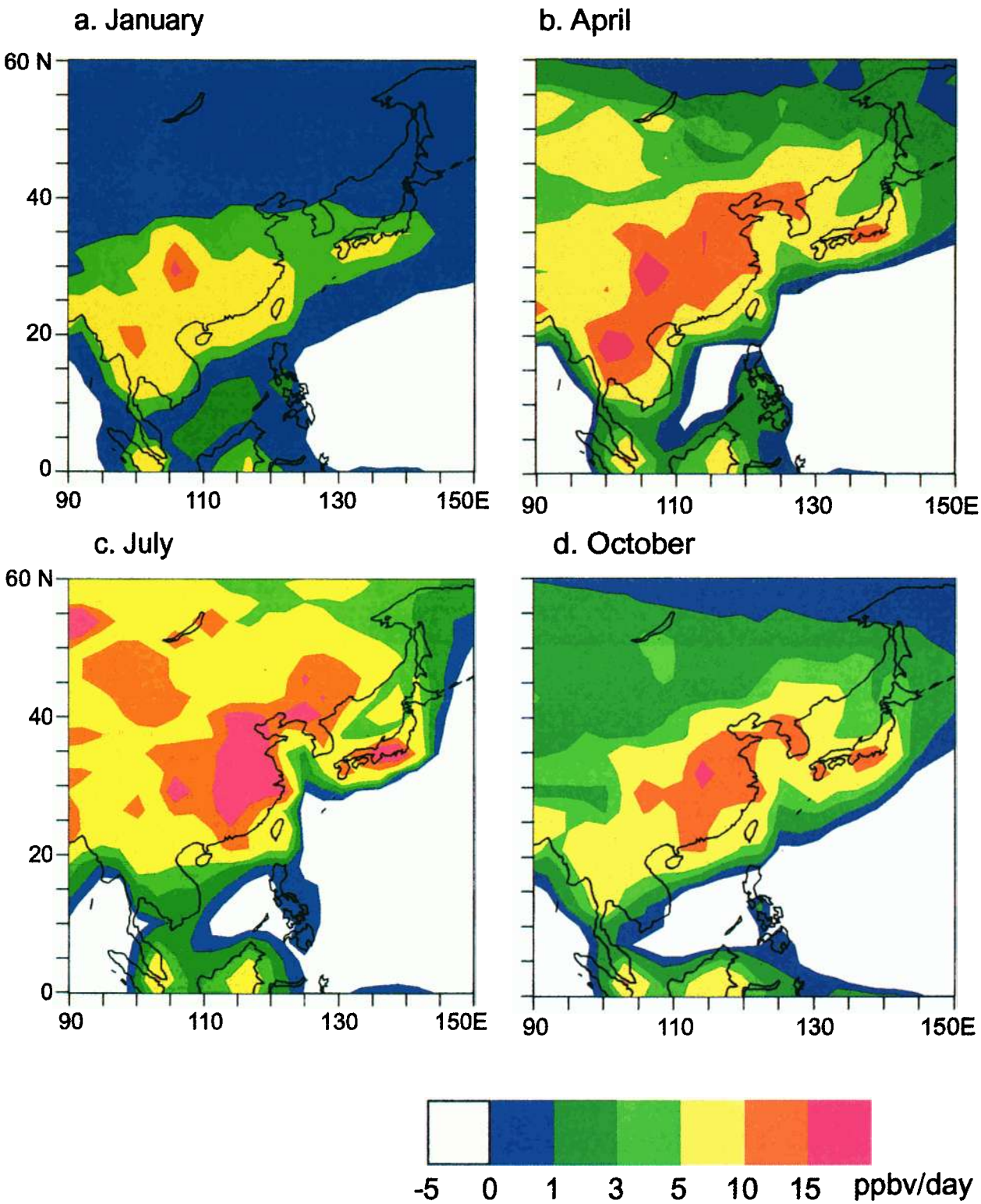

Plate 1. Net ozone production over East Asia in (a) January, (b) April, (c) July, and (d) October calculated by MOZART 1. Results are boundary layer (0-2.1 km) means. Units are ppbv/d.

adequately simulates photochemical O_3 production. Since CO serves as a good tracer of combustion, correlation between O_3 and CO is often used for evaluating photochemical O_3 production [e.g., *Parrish et al.*, 1993; *Andreae et al.*, 1994]. We compared the slopes of the correlations obtained using least squares regressions of O_3 versus CO for Oki and Happo. Figure 2 shows monthly values of the correlation slope from both the model and observations. Model results in Figure 2 use 24-hour means of O_3 and CO mixing ratios in the boundary layer (approximately 0-2.1 km). Measurement points are averages of afternoon mixing ratios (1300-1700 LT) when the boundary layer is well mixed. Figure 2 shows a general agreement between the O_3 to CO correlations obtained from model results and measurements for both sites throughout the year with the exception of winter. The seasonal pattern, particularly for Oki, agrees reasonably well with the observed correlations. These results suggest photochemical O_3 production is relatively well reproduced by the model in the region of East Asia.

3. Geographical and Seasonal Distributions of Photochemical O_3 Production Over East Asia

The effect of regional photochemistry on O_3 is defined by the production and loss rates of the odd oxygen family (O_x = $O_3 + O(^1D) + O(^3P) + NO_2 + 2 \times NO_3 + 3 \times N_2O_5 + HNO_3 + HNO_4 + PAN$). We take the production and loss of odd oxygen species (O_x) as equivalent to the production and loss of O_3. This definition accounts for the rapid cycling between O_3 and other forms of odd oxygen species.

Plate 1 shows the geographical distribution of net O_3 production in East Asia in January (Plate 1a), April (Plate 1b), July (Plate 1c), and October (Plate 1d) in the boundary layer (approximately 0-2.1 km) as calculated by MOZART 1. Results are presented as monthly averages. Net O_3 production is obtained by subtracting photochemical loss from photochemical production. Plate 1 indicates that net O_3 production generally takes place over continental East Asia where emissions of O_3 precursors are high. Over the oceans, O_3 destruction generally exceeds O_3 production because of low NO_x concentrations.

The seasonal variation in net O_3 production over East Asia is strongly influenced by seasonal changes in transport. Figure 3 shows monthly mean CCM-2.5 wind fields at 929, 695, and 408 hPa in January (Figure 3a), April (Figure 3b), July (Figure 3c), and October (Figure 3d). We divide the region into three different transport regimes: (1) north of 20°N, (2) between 5°N and 20°N, and (3) south of 5°N.

As shown in Figure 3, north of 20°N in the mid and upper troposphere strong northwesterly continental outflow occurs in January, April, and October. In July, westerly winds weaken, and southeasterly monsoons dominate as far north as 30°N. In the boundary layer, strong west north-westerlies prevail north of 40°N in January, April, and October. Between 20°N and 40°N, wind direction is mixed. In July, onshore winds dominate between 20°N and 40°N with winds north of 40°N being weak and primarily from the southwest.

Plate 1 shows that north of 20°N O_3 production is largest in summer and lowest in winter reflecting the seasonal change in insolation and photochemical activity. From spring to fall, active production occurs over an extensive area from the east coast of China to the Japanese mainland, which we ascribe to large anthropogenic emissions in this area. In July, net O_3 production reaches a maximum (over 15 ppbv/d) over central China, Korea, and the Japanese mainland; O_3 production rates of over 5 ppbv/d occur over most of mainland China during this season. In January, while net O_3 production in the region north of 30°N becomes lower compared to other months, O_3 production rates of 5-10 ppbv/d persist between 20°N and 30°N. A strong gradient in photochemical activity at 30°N in winter has been observed by *Crawford et al.* [1997] in an analysis of PEM-West B data. They found a markedly lower tropopause height and higher total O_3 column north of 30° N which lead to greatly reduced rates of net O_3 production. This sharp decrease in the height of the tropopause and increase in total O_3 column north of 30° N is reproduced in our MOZART 1 simulation.

From 5°N to 20°N over the Indochina peninsula, northeasterly winds predominate in January, April, and October, while southwesterly monsoons bring moist air from the Indian Ocean to the region in July. The seasonal variation in O_3 production in this region is characterized by the wet (July–October) and dry (December–April) seasons. In the wet season, clean oceanic air from the Indian Ocean brings air low in O_3 and O_3 precursors into the region, while in the dry season ozone concentrations greatly increase due to regional biomass burning which is generally most intense at the end of the dry season [*Hao and Liu*, 1994]. Figure 4 shows the average monthly emissions of CO from the Indochina Peninsula (12.6°-20.9° N, 98.4°-109.7° E) in MOZART with maximum emissions occurring in April. Maximum O_3 production (over 15 ppbv/d) also occurs in April and is shown in Plate 1. In this region, higher rates of O_3 production occur in January than in July or October. Long-range transport of continental air does not appear to characterize ozone concentrations in this region

In tropical Asia, between 5°N and 5°S, southeasterly winds predominate in the boundary layer throughout the year. In the mid and upper troposphere, weak westerlies occur in January and April, while stronger westerlies occur in July and October with a convergence of easterlies and westerlies over peninsular Malaysia in the upper troposphere during July. Plate 1 indicates that photochemical production of O_3 does not exhibit a noticeable seasonal cycle in this region because there is not a significant seasonal cycle in either insolation or emissions.

We examined seasonal O_3 budgets for East Asia by quantifying O_3 production, loss, and deposition. We estimated deposition fluxes by multiplying the deposition velocities by the O_3 concentrations in the surface layer of MOZART 1. The horizontal extent of the region is shown in Figure 5. Figure 6 shows the seasonal variation in net photochemical production, loss, and deposition of O_3 in the boundary layer (0-2.1 km) over East Asia. These figures present net O_3 production as the difference between O_3 chemical production and loss. Seasonal variations of photochemical production and loss of O_3 both have a maximum in summer and a minimum in winter. Deposition also has a maximum in summer, which is explained by the additional vegetation available for O_3 uptake during the summer. Our annual net O_3 production in the boundary layer over East Asia of 117 Tg/yr is in good agreement with an estimate by *Jaffe et al.* [1996] of 100 Tg/yr, which was obtained from a regression analysis of NO_y and O_3 measurements at Oki Island and NO_x emissions from East Asia (China, Taiwan, Korea, and Japan) given by *Kato and Akimoto* [1992].

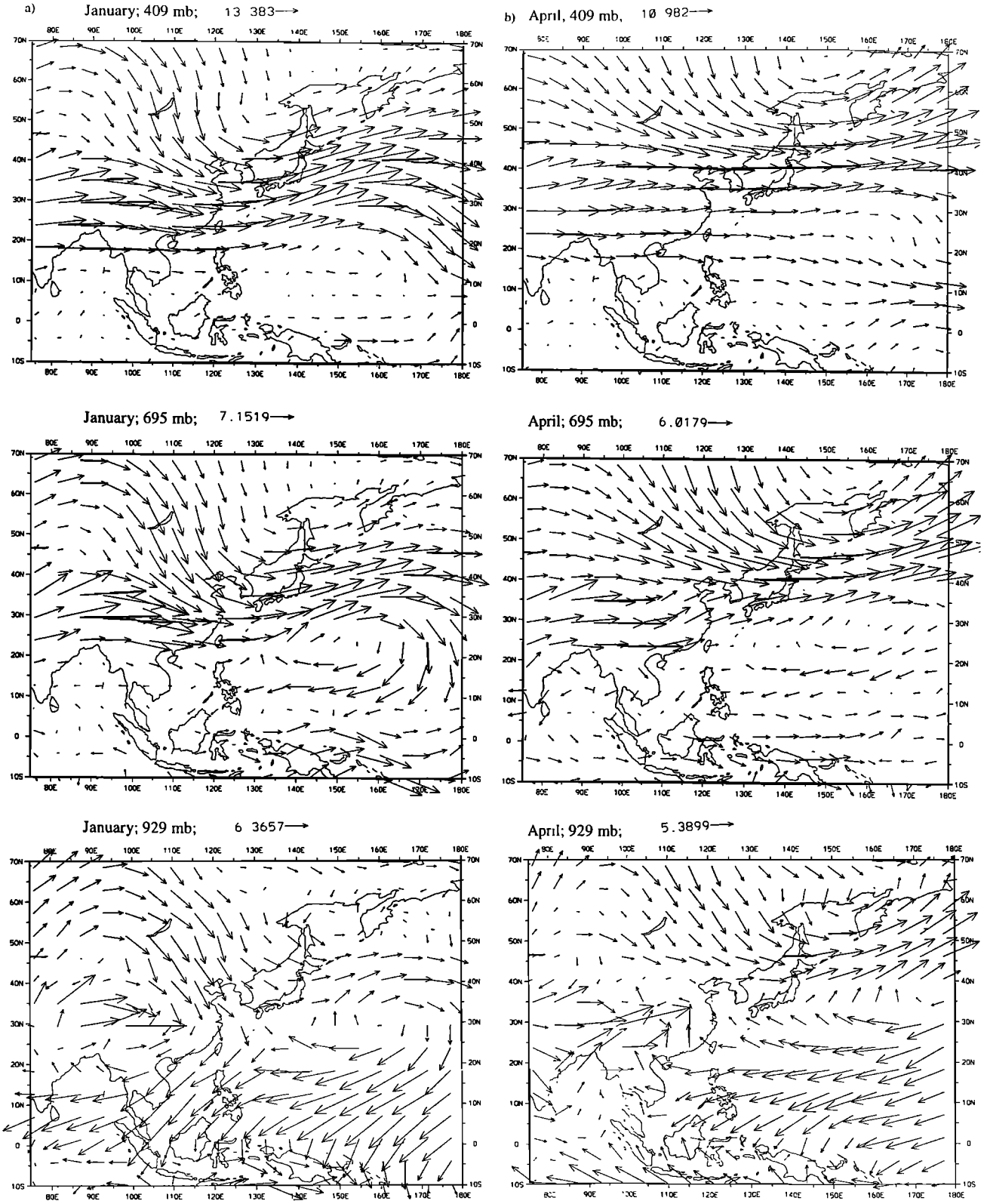

Figure 3. Monthly average wind vector plots over East Asia from CCM2 (library Ω0.5) winds at the surface (925 mbar), midtroposphere (695 mbar), and the upper troposphere (409 mbar) in (a) January, (b) April, (c) July, and (d) October. Winds on any given day of a month may deviate from the average monthly winds plotted here.

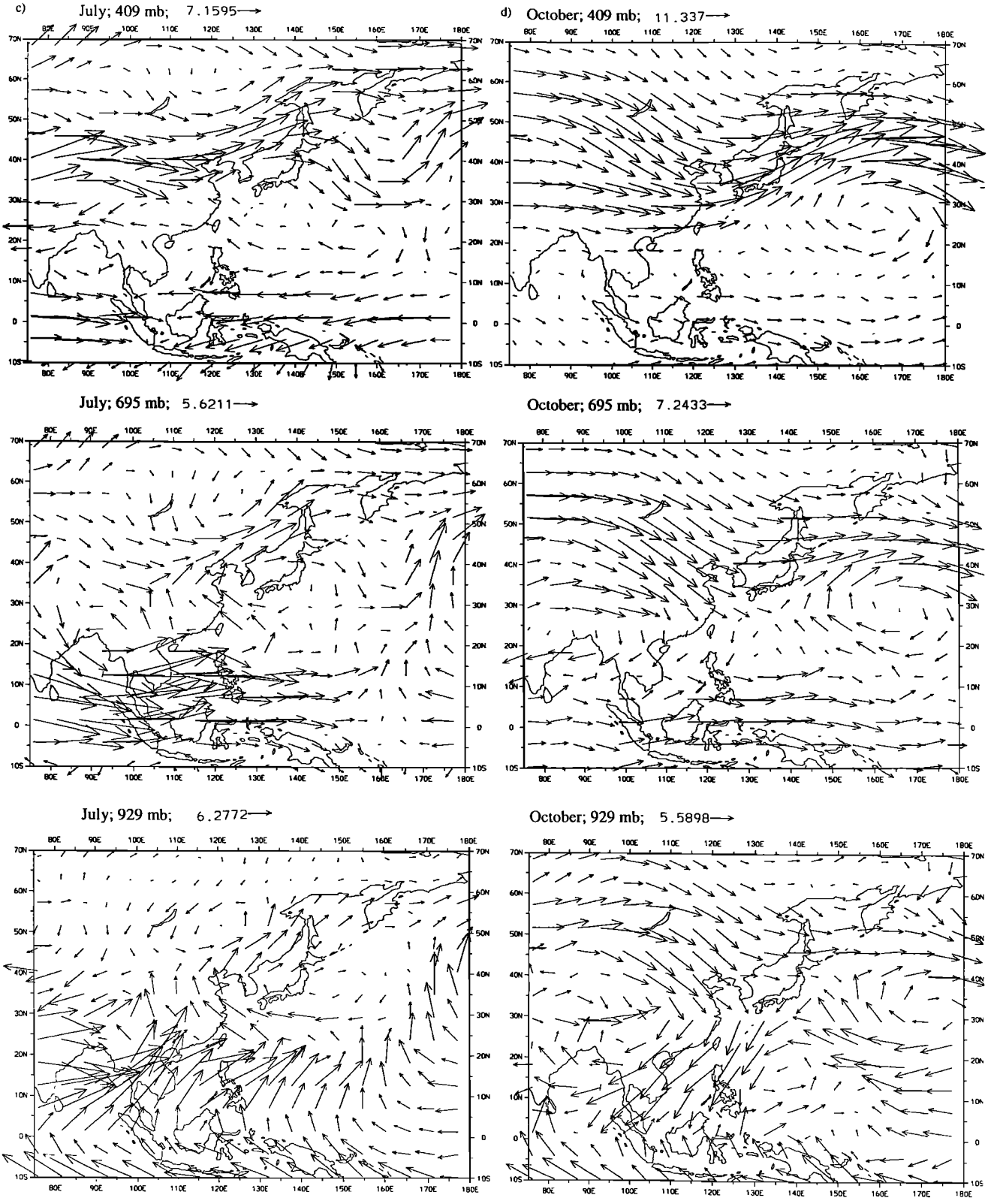

Figure 3. (continued)

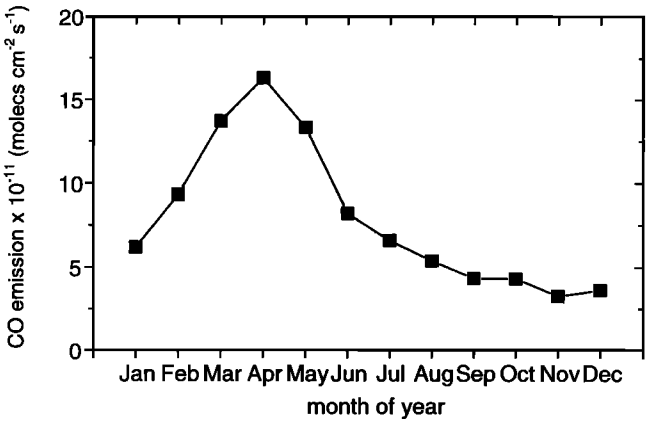

Figure 4. Seasonal variation of mean surface CO flux out of Indochina Peninsula (12.6°-20.9°N, 98.4°-109.7°E) from MOZART 1.

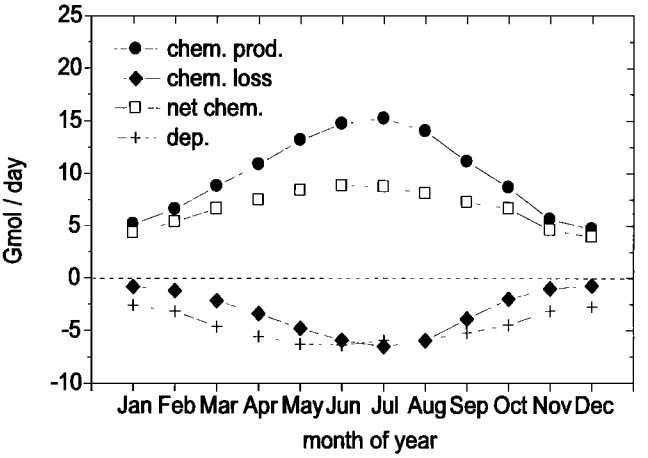

Figure 6. Seasonal variations of chemical production (chem. prod.), chemical loss (chem. loss), net chemical production (net chem.) and dry deposition (dep.) of ozone in the boundary layer (0-2.1 km) of East Asia. Units are Gmol/day.

Figure 7 shows seasonal variations of net O_3 production over East Asia in three altitude regions: the boundary layer (surface to 2.1 km), the mid troposphere (2.1-5.7 km), and the upper-troposphere (5.7-9.0 km). Figure 7 indicates net O_3 production is largest in the boundary layer, lowest in the midtroposphere, and of intermediate value in the upper troposphere. The boundary layer and upper troposphere both show a broad summer maximum, while the midtroposphere exhibits a slight spring maximum. This profile and seasonal cycle can be explained by the fact that the highest concentrations of O_3 precursors are found in the polluted continental boundary layer and, in both model and observations, NO (a primary precursor for O_3 production) vertical profiles exhibit maximum mixing ratios in the upper troposphere [*Hauglustaine et al.*, 1998a]. Higher O_3 production in the upper free troposphere than in the midtroposphere has also been reported in a variety of other model studies [*Liu et al.*, 1980; *Jacob et al.*, 1996; *Davis et al.*, 1996; *Berntsen and Isaksen*, 1997; *Yienger et al.*, 1999]. The spring maximum of net O_3 production in northern midlatitudes has been noted by *Beekman et al.* [1994] from climatological analysis and by *Yienger et al.* [1999] using the Geophysical Fluid Dynamics Laboratory (GFDL) global model. Our springtime maximum in net O_3 production over Asia in the midtroposphere with MOZART are similar to those obtained with the GFDL model. However, according to our simulations, the springtime maximum in O_3 mixing ratio that is observed at Oki and Happo (see Figure 1) cannot be accounted for by photochemistry alone. The discrepancy between the observed and modeled concentration in winter and spring most likely is due to the under-representation of the influx of stratospheric O_3 in MOZART 1, as noted earlier. According to this interpretation the stratospheric component would have a rather broad maximum from winter to spring. The combination of this stratospheric influx with a sharp increase of photochemical buildup of ozone from February to May, as shown in Figure 1, can explain the observed spring maximum in April and May at Oki and Happo.

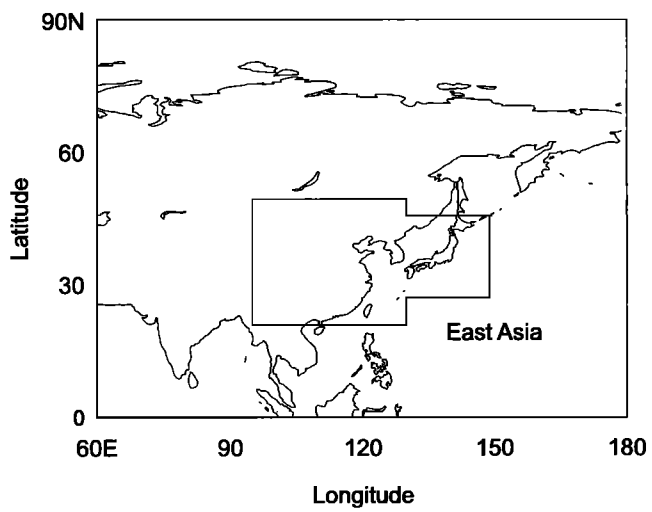

Figure 5. Geographical boundaries of East Asia used in the analysis.

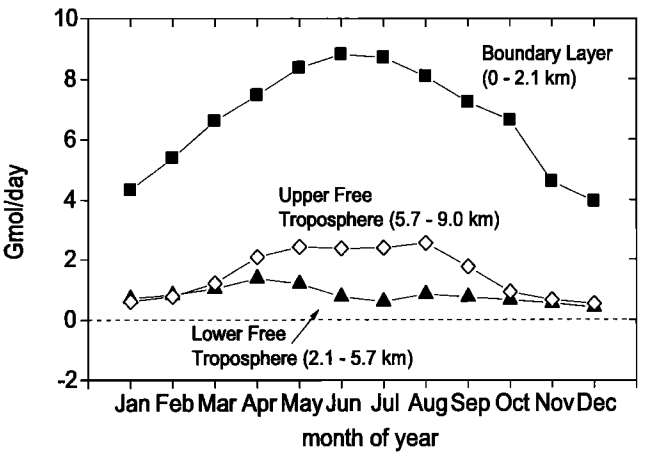

Figure 7. Seasonal variation of net chemical ozone production for East Asia in the boundary layer (surface to 2.1 km), the midtroposphere (2.1-5.7 km), and upper troposphere (5.7-9.0 km).

4. Export of O_3 and Its Precursors From East Asia

Figure 6 indicates a net production of O_3 in the boundary layer of East Asia throughout the year. Since O_3 produced from net chemistry exceeds deposition, we can infer that the East Asian boundary layer is a net exporter of O_3 in all seasons. One approach to examining O_3 export from a particular region is to use O_3 to CO correlations [*Parrish et al.*, 1993; *Chin et al.*, 1994; *Mauzerall et al.*, 1996; *Atherton et al.*, 1996; *Hauglustaine et al.*, 1998b]. CO serves as a tracer of combustion, and O_3 is formed from combustion byproducts (NO_x, hydrocarbons, and CO). Thus, in air parcels aged from a few days to a week, the slope of the O_3 to CO correlation indicates the quantity of O_3 produced per CO molecule emitted. Using this relationship, *Parrish et al.* [1993] have calculated the O_3 flux out of North America from measurements off the east coast of Canada and CO emissions in the United States east of the Mississippi River. They estimated 1.1 Gmol/d of O_3 is transported from North America to the Atlantic Ocean in summer. However, their estimate is considered lower than the real O_3 export from this region because in addition to direct emissions of CO, a significant amount of CO is produced from the oxidation of hydrocarbons [*Chin et al.*, 1994].

Here we investigate the geographical variation of O_3/CO correlations in the East Asian boundary layer to describe the export of photochemically produced O_3 from this region. A similar approach was taken by *Atherton et al.* [1996] in model studies of O_3 transport and photochemistry over the North Atlantic Ocean. Plates 2 and 3 show seasonal mixing ratios of O_3 and CO in the East Asian boundary layer, respectively. The influence of the summer monsoon is evident in the steep gradient of O_3 and CO just east of Japan in July. Plate 4 shows horizontal distributions of O_3/CO regression slopes calculated from 24-hour averages of each grid cell in the boundary layer column (0-2.1 km) in January (Plate 4a), April (Plate 4b), July (Plate 4c), and October (Plate 4d). Figure 8 gives an example of how scatter plots of daily values of O_3 and CO mixing ratios in a model grid cell column of the boundary layer centered at (26.5°N,136.4°E) were used over the course of a month to obtain the values used in Plate 4.

Plate 4 clearly shows seasonal variations of slope values which have a maximum in summer (July) and a minimum in winter (January), due to seasonal changes in photochemical activity. In January, O_3/CO correlations north of 30°N are below 0.1 and statistically insignificant in most regions, while in July correlation slopes over 0.3 appear even in some areas north of 40°N. Such slope values in July agree well with reported values for observations in North America in summer (Table 1). Plate 4c shows high slope values (over 0.5) south of Japan. However, these high positive correlations are not likely to be caused by pollution transport since CO concentrations are low in this area (see Plate 3c). High positive O_3/CO correlations are not a common feature in clean background air. Rather, O_3 and CO in background air tend to show negative correlations because of air mass alternation between lower tropospheric air (high in CO and low in O_3) and upper tropospheric air (low in CO and high in O_3) [*Fishman and Seiler*, 1983]. In the present case in Plate 4, one explanation of high positive correlations in low CO regions is depletion of both O_3 and CO in tropical air because the lifetime of CO is relatively short (about 20 days) in tropical summer [*Mauzerall et al.*, 1998]. Although Figure 3 shows that average winds in the boundary layer in July are coming from the east, occasional intrusions of continental air to the Pacific in summer [*Tsutsumi et al.*, 1998; *Pochanart et al.*, 1999] could provide the occasionally higher O_3 and CO mixing ratios which create the correlation.

Horizontal distributions of O_3/CO correlations reflect both regional photochemical activity and transport. As is shown in Figure 3, along the coast of east Asia north of 35°N, continental outflow prevails from fall to spring with maximum outflow in winter [*Hoell et al.*, 1997; *Merrill et al.*, 1989, 1997]. This outflow is carried around the high-pressure system centered at 30°N, 160°E first east and then south into a region of higher insolation and more active photochemistry. Plate 4a shows an increase in slope values from inland to offshore Asia south of 30°N in January. This progression occurs because O_3 continues to be produced in air masses as they are transported first east and then south around the high-pressure system off the Asian coast. Plate 1 indicates a gradient of continuing O_3 production east of continental Asia and Japan.

Continental outflow also influences O_3/CO correlations in April and October. Plates 4b and 4d show a gradual increase of slope values from inland to offshore as in Plate 4a for January, although features are more complex in these months. Higher positive O_3 and CO correlations appear in April in the boundary layer over the ocean in spite of onshore winds as far north as 35° N as shown in Figure 3b. However, as is also shown in Figure 3b, in April strong westerlies exist just above the boundary layer over continental Asia as far

Table 1. Reported O_3/CO Correlation Values From Observations in North America and in Japan

ΔO3/ΔCO	Location	Season	Reference
0.40a	U.S. east coast	Aug.Sept.	*Anderson et al.* [1993]
0.28-0.32	U.S. flatland sites	June-Aug.	*Chin et al* [1994, and references therein]
0.27	Bermuda islands, U.K.	March-June	*Dickerson et al.* [1995]
0.25	western North Atlantic	Aug.	*Daum et al.* [1996]
0.5 ± 0.5b	eastern Canada	July-Aug.	*Mauzerall et al.* [1996]
0.3-0.4	Atlantic coast of Canada	Jul-Sept.	*Parrish et al.* [1998]
0.11-0.23	Oki, Japan	June-Aug.	*Pochanart et al.* [1999]
0.09-0.16	Happo, Japan	June-Aug.	*Kajii et al.* [1998]

[a] For polluted air masses.

[b] Aged pollution plumes.

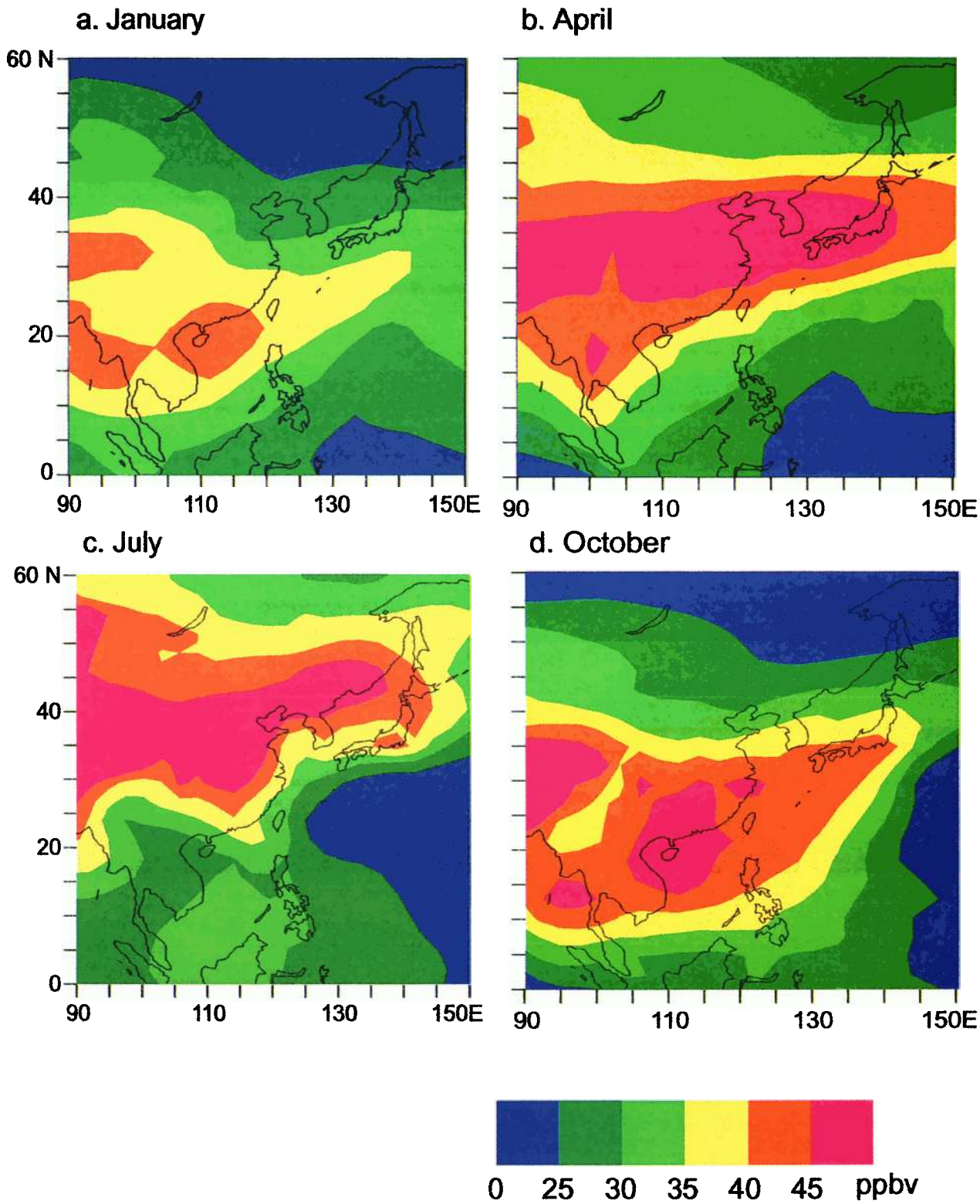

Plate 2. Horizontal variations of monthly mean O_3 mixing ratios in the boundary layer (0-2.1 km) for (a) January, (b) April, (c) July, and (d) October.

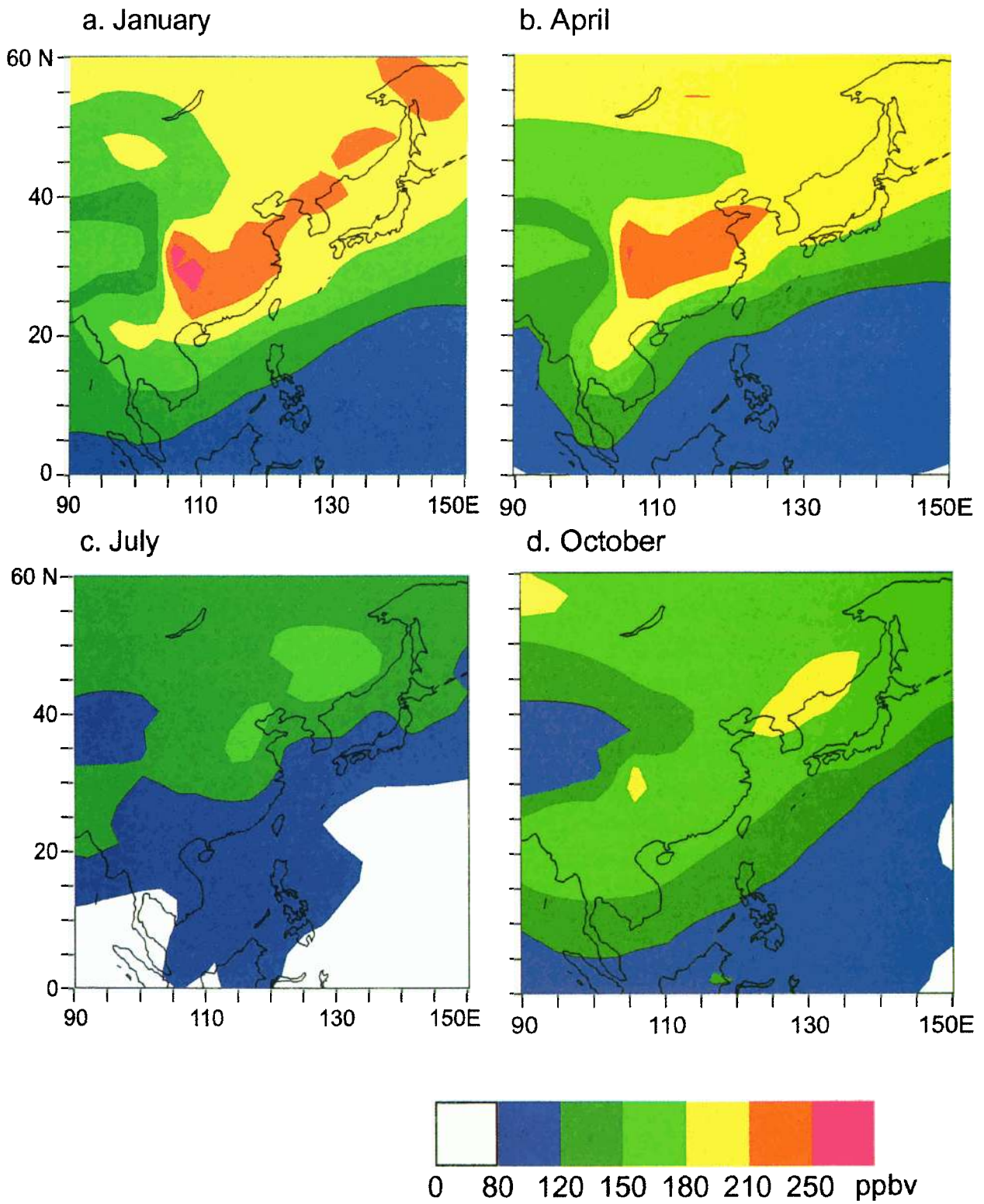

Plate 3. Horizontal variations of monthly mean CO mixing ratios in the boundary layer (0-2.1 km) for (a) January, (b) April, (c) July, and (d) October.

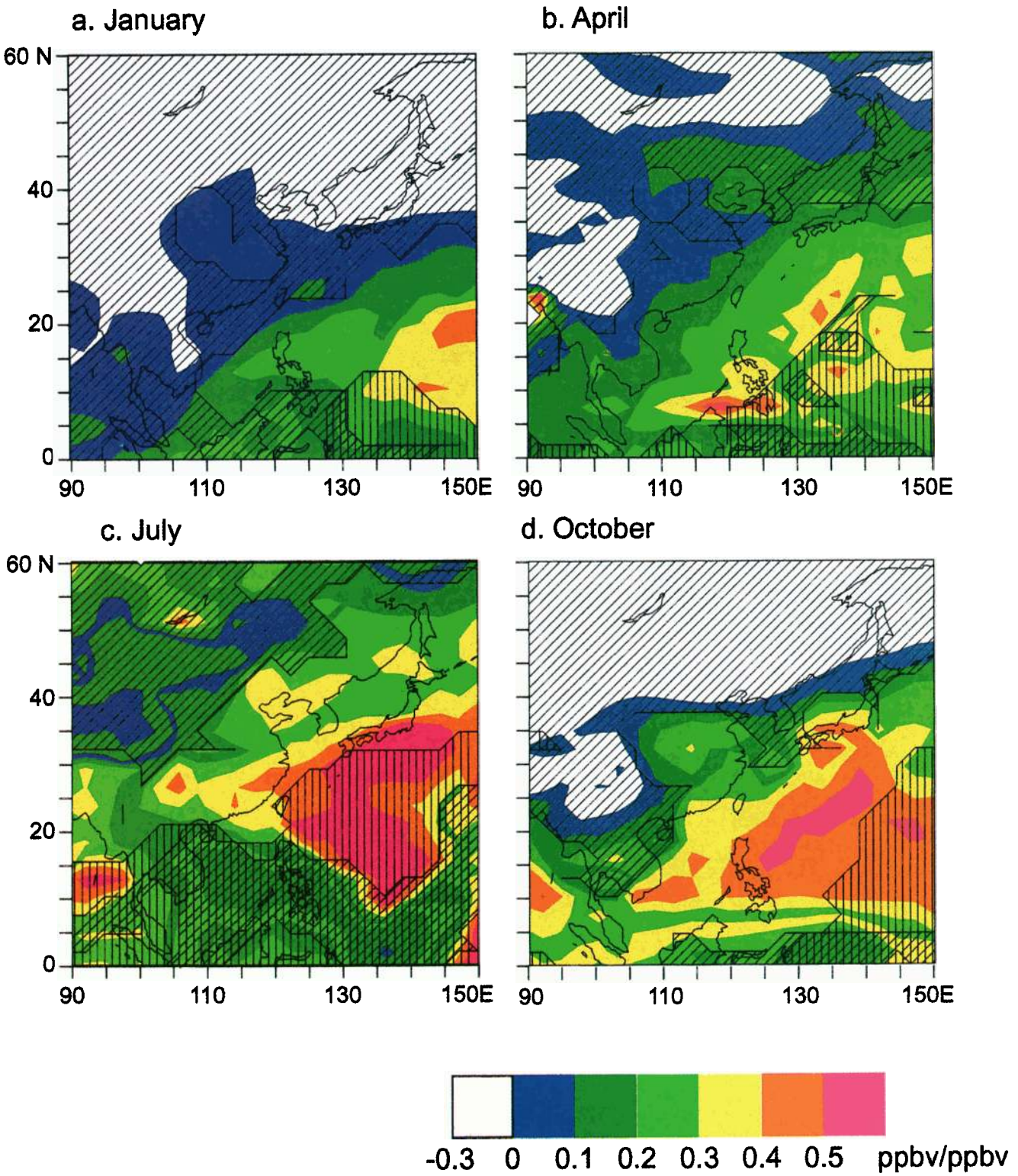

Plate 4. Horizontal variations of the O_3/CO correlation slope for (a) January, (b) April, (c) July, and (d) October. Calculation is based on boundary layer (0-2.1 km) means. Areas covered with oblique lines are those where correlation coefficients r^2 are below 0.3 or t tests have yielded less than 95% confidence limits so that O_3/CO correlations are not considered to be statistically significant. Vertical lines on Plate 4 cover areas where CO<100 ppbv indicating relatively clean marine air which is unlikely to have been significantly influenced by continental outflow.

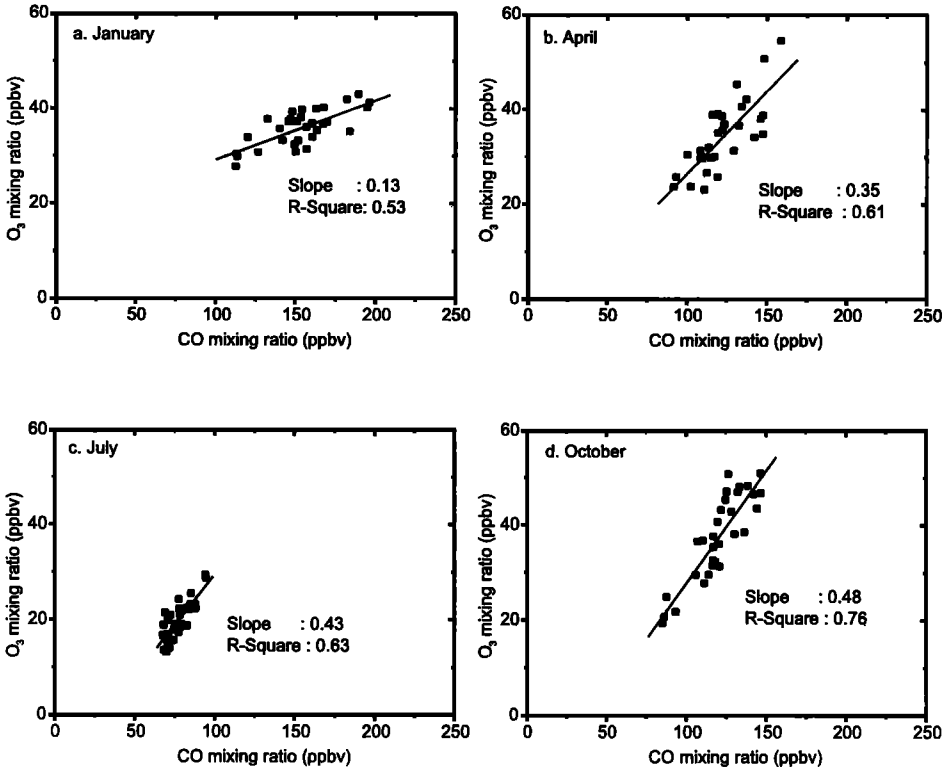

Figure 8. Scatterplots of monthly O_3 and CO data in a model grid cell centered at (26.5°N, 136.4°E) for (a) January, (b) April, (c) July, and (d) October. Each point on the plot represents a 24-hour daily average of model-calculated O_3 and CO concentrations.

south as 25°N and transport anthropogenic emissions to the east. October is a month when the influence of continental outflow is weak over the Pacific Ocean [*Hoell et al.*, 1996; *Bachmeier et al.*, 1996]. However, along the East Asian coast, anticyclones over China result in occasional transport of pollution from the continental region to the Pacific [*Bachmeier et al.*, 1996; *Akimoto et al.*, 1996; *Pochanart et al.* 1999]. Figure 3d shows this anticyclonic flow over south central Asia above the East Asian coastal region, and Plate 4d shows a gradient of correlation slope values to the south-east.

In summer, clean oceanic air is transported to continental Asia from the south-east (as shown in Figure 3c). Plate 4c shows that starting just east of the Asian coast, the boundary layer over the Pacific Ocean has CO mixing ratios below 100 ppbv because of on-shore flow of clean background marine air. In summer, export of pollution from Asia does not take place in the east/southeast directions. Instead, as indicated in Figure 3c, O_3 export from the Asian boundary layer could occur to the north/northeast, or additionally via vertical advection or convection. O_3/CO correlation slopes above 0.3 in northeastern Asia support the hypothesis that pollution may be advected to the northeast. The direction of export fluxes from Asia is being examined in detail using MOZART, version 2 which archives mass fluxes across grid cell boundaries for a variety of tracers [*Mauzerall et al.*, 1999].

O_3/CO correlations have been extensively investigated over the east coast of North America. Reported values of correlation slopes (see Table 1) range from 0.25-0.5 in summer. *Kajii et al.* [1998] and *Pochanart et al.* [1999] also examined O_3/CO correlations at the remote Oki and Happo, Japan, sites using the same data which we use here to compare with model values. They found O_3/CO correlation slopes ranging from 0.09-0.23 in summer which are consistent with MOZART values for Oki and Happo shown in Figure 2, although they differ in averaging periods. These values are significantly lower than those reported for eastern North America in the same season. Seasonal variations in transport regimes over Asia clearly have a strong influence on O_3 export from Asia. Plate 1 indicates maximum O_3 production in July, but O_3/CO correlation slopes shown in Plate 4 indicate that in July eastward export is limited to central and northern Japan and onshore winds bring clean air close to continental Asia.

Using the O_3/CO enhancement ratio of 0.3, which is a typical value downwind of the Asian continent in Plate 4 except in January, we can roughly estimate O_3 export out of the East Asian boundary layer. Multiplying the O_3/CO enhancement ratio by the CO emission of 11 Gmol/d which is the annual mean CO surface flux in MOZART 1 from the East Asian region shown in Figure 5, an upper estimate of 3.3 Gmol/d (58 Tg/yr) of O_3 export from East Asia is obtained. This is approximately half of the 117 Tg/yr of O_3 estimated to be photochemically produced in the East Asian boundary layer, and is slightly less than 70% of the net production of pollution O_3 that was estimated by *Liang et al.* [1998] to be exported from the U.S. boundary layer in summer. The technique employed here is more suited for a continental region that is always ventilated in the same direction. In Asia the direction of export varies seasonally, and further research

is needed to determine in which direction O_3 is transported, as well as to obtain a more robust estimate of the magnitude of export. While the present analysis only considered horizontal transport by examining horizontal variation of O_3/CO correlations, O_3 which is produced in the boundary layer could be exported vertically as well. *Jacob et al.* [1993] concluded O_3 export out of the U.S. boundary layer is principally by vertical transport to the free troposphere. In further work, quantitative estimates of vertical and horizontal O_3 export will be obtained using MOZART, version 2. In addition, an assessment of the export of O_3 precursors which may significantly contribute to in situ production of O_3 downwind of source regions will also be conducted [*D.L. Mauzerall et al.*, manuscript in preparation, 2000].

5. Conclusions

We have examined seasonal geographical distributions of tropospheric O_3 production and mixing ratios over East Asia with a global three-dimensional chemical transport model called MOZART 1. In comparison with observational data at remote Japanese sites, we found the model underestimates O_3 concentrations by 10-20 ppbv from winter to spring, but reproduces measurements reasonably well in summer. It provides reasonable agreement in O_3/CO correlations throughout the year at both sites giving us confidence that photochemical production of O_3 is relatively well reproduced by MOZART in the region of east Asia.

Geographical distributions of net O_3 production over East Asia indicate that there are three major types of seasonal dependence according to latitude (north of 20°N, 5°N-20°N, and south of 5°N). North of 20°N, O_3 production is largest in summer and lowest in winter reflecting the seasonal change in insolation and photochemical activity. In this region, net ozone production from spring through autumn is found to have a maximum extending from 25°N-40°N and from central eastern China to Japan, resulting from the strong emission and transport of anthropogenic O_3 precursors. In winter, maximum O_3 production in this region occurs between 20°N and 30°N due to both local emissions and transport of O_3 precursors from northeast China into this region via the prevailing high- pressure system off the coast of Asia. Over the Indochina peninsula, between 5°N and 20°N, net O_3 production is controlled by the seasonal cycle between wet and dry seasons and has a maximum at the end of the dry season due to emissions from biomass burning. South of 5°N, in the true tropics, O_3 mixing ratios are relatively constant throughout the year and do not exhibit a seasonal cycle. A spring-summer maximum of net O_3 production is found throughout the troposphere over East Asia. We estimate an annual net O_3 production in East Asia of 117 Tg/yr.

In the boundary layer and upper troposphere, net O_3 production has a broad maximum in summer, while in the mid-troposphere, net O_3 production is much weaker and has a slight spring maximum over East Asia. O_3/CO correlations off the east coast of the Asian continent show strong horizontal variability driven by both photochemical activity and meteorology. Using an O_3/CO enhancement ratio of 0.3, which is a typical value downwind of the Asian continent, an upper estimate of O_3 export from East Asia to the Pacific Ocean in the mid-1980s of 3.3 Gmol/d (58 Tg/yr) is obtained.

Acknowledgements. The authors thank P. Pochanart, Y. Kajii, J. Hirokawa, K. Someno, H. Tanimoto, M. Nakao, and T. Katsuno for the use of unpublished observational data from Oki and Happo, Japan. This research has been supported by an Advanced Study Program postdoctoral fellowship from the National Center for Atmospheric Research to D. Mauzerall and by Core Research for Environmental Science and Technology (CREST) of the Japan Science and Technology Corporation. The National Center for Atmospheric Research is operated by the University Corporation for Atmospheric Research under sponsorship of the National Science Foundation.

References

Akimoto, H., et al., Long-range transport of ozone in the East Asian Pacific rim region, *J. Geophys. Res., 101*, 1999-2010, 1996.

Anderson, B. E., G. L. Gregory, J. D. W. Barrick, J. E. Collins, Jr., G. W. Sachse, D. Bagwell, M. C. Shipham, J. D. Bradshaw, and S. T. Sandholm, The impact of U.S. continental outflow on ozone and aerosol distributions over the western Atlantic, *J. Geophys. Res., 98*, 23447-23489, 1993.

Andreae, M. O., B. E. Anderson, D. R. Blake, J. D. Bradshaw, J. E. Collins, G. L. Gregory, G. W. Sachse, and M. C. Shipham, Influence of plumes from biomass burning on atmospheric chemistry over the equatorial and tropical South Atlantic during CITE 3, *J. Geophys. Res., 99*, 1,2793-1,2808, 1994.

Atherton, C. S., S. Sillman, and J. Walton, Three-dimensional global modeling studies of the transport and photochemistry over the North Atlantic Ocean, *J. Geophys. Res., 101*, 2,9289-2,9304, 1996.

Bachmeier, A. S., R. E. Newell, M. C. Shipham, Y. Zhu, D. R. Blake, and E. V. Browell, PEM-West A: Meteorological overview, *J. Geophys. Res., 101*, 1655-1677, 1996.

Beekman, M., G. Ancellet, and G. Megie, Climatology of tropospheric ozone in southern Europe and its relation to potential vorticity, *J. Geophys. Res., 99*, 1,2841-1,2853, 1994.

Benkovitz, C. M., M. T. Sholtz, J. Pacyna, L. Tarrason, J. Dignon, E. C. Voldner, P. A. Spiro, J. A. Logan, and T. E. Graedel, Global gridded inventories of anthropogenic emissions of sulfur and nitrogen, *J. Geophys. Res., 101*, 2,9239-2,9253, 1996.

Berntsen, T. K., and I. S. A. Isaksen, A global three-dimensional chemical transport model for the troposphere, 1, Model description and CO and ozone results, *J. Geophys. Res., 102*, 21239-21280, 1997.

Berntsen, T., I. S. A. Isaksen, W.-C. Wang, and X.-Z. Liang, Impacts of increased anthropogenic emissions in Asia on tropospheric ozone and climate, a global 3-D model study, *Tellus,Ser. B,48B*, 13-32, 1996.

Berntsen, T. K., S. Karlsdottir, and D.A. Jaffe, Influence of Asian emissions on the composition of air reaching the northwestern United States, *Geophys. Res. Lett, 26*, 2171-2174, 1999.

Brasseur, G. P., J. T. Kiehl, J. -F. Müller, T. Schneider, C. Granier, X. Tie, and D. Hauglustaine, Past and future changes in global tropospheric ozone: Impact on radiative forcing, *Geophys. Res. Lett., 25*, 3807-3810, 1998a.

Brasseur, G. P., D. A. Hauglustaine, S. Walters, P. J. Rasch, J. -F., Müller, C. Granier, and X. X. Tie, MOZART, a global chemical transport model for ozone and related chemical tracers, 1, Model description, *J. Geophys. Res., 103*, 28,265-28,289, 1998b.

Brasseur, G.P., X.X. Tie, P. Rausch, and F. Lefèvre, A three-dimensional simulation of the Antarctic ozone hole: Impact of anthropogenic chlorine in the lower stratosphere and upper troposphere, *J. Geophys. Res.,102*, 8909-8930, 1997.

Carmichael, G. R., I. Uno, M. J. Phadnis, Y. Zhang, and Y. Sunwoo, Tropospheric ozone production and transport in the springtime in East Asia, *J. Geophys. Res., 103*, 10,649-10,671, 1998.

Chameides, W. L., P. S. Kasibhatla, J. Yienger, and H. Levy II, Growth of continental-scale metro-agro-plexes, regional ozone pollution and world food production, *Science, 264*, 74-77, 1994.

Chin, M., D. J. Jacob, J. W. Munger, D. D. Parrish, and B. G. Doddridge, Relationship of ozone and carbon monoxide over North America, *J. Geophys. Res., 99*, 14,545-14,573, 1994.

Crawford, J., et al., An assessment of ozone photochemistry in the extratropical western North Pacific: Impact of continental outflow during the late winter/early spring, *J. Geophys. Res., 102*, 28,469-28,487, 1997.

Daum, P. H., L. I. Kleinman, L. Newman, W. T. Luke, J. Weinstein-Lloyd, C. M. Berkowitz, and K. M. Busness, Chemical and physical properties of plumes of anthropogenic pollutants transported over the North Atlantic during the North Atlantic Regional Experiment, *J. Geophys. Res., 101*, 29,029-29,042, 1996.

Davis, D. D. , et al., Assessment of ozone photochemistry in the western North Pacific as inferred from PEM-West A observations during the fall 1991, *J. Geophys. Res., 101*, 2111-2134, 1996.

Dickerson, R. R., B. G. Doddridge, P. Kelley, and K. P. Rhoads, Large-scale pollution of the atmosphere over the remote Atlantic Ocean: Evidence from Bermuda, *J. Geophys. Res., 100*, 8945-8952, 1995.

Emmons, L. K., et al., Climatologies of NO_x and NO_y: A comparison of data and models, *Atmos. Environ., 31*, 1851-1904, 1997.

Fishman, J., and W. Seiler, Correlative nature of ozone and carbon monoxide in the troposphere: Implications for the tropospheric ozone budget, *J. Geophys. Res., 88*, 3662-3670, 1983.

Fishman, J., V. Ramathan, P. J. Crutzen, and S. C. Liu, Tropospheric ozone and climate, *Nature, 282*, 818-820, 1979.

Hack, J. J., Parameterization of moist convection in the National Center for Atmospheric Research community climate model (CCM2), *J. Geophys. Res., 99*, 5551-5568, 1994.

Hao, W. M., and M.-H. Liu, Spatial and temporal distribution of tropical biomass burning, *Global Biogeochem. Cycles, 8*, 495-503, 1994.

Hauglustaine, D. A., G. P. Brasseur, S. Walters, P. J. Rasch, J.-F., Müller, L. K. Emmons, and M. A. Carroll, MOZART, a global chemical transport model for ozone and related chemical tracers, 2, Model results and evaluation, *J. Geophys. Res., 103*, 28,291-28,335, 1998a.

Hauglustaine, D.A., G.P. Brasseur, and S. Walters, A three-dimensional simulation of ozone over the North Atlantic Ocean, in: *Atmospheric Ozone: proceedings of the XVIII Quadrennial Ozone Symposium, 1996 and Tropospheric Ozone Workshop*, L'Aquila, Italy 12-21 September 1996, edited by Reuben D. Bojkov, Guido Visconti, 1998b.

Heck, W. W., W. W. Cure, J. O. Rawlings, L. J. Zaragoza, A. S. Heagle, H. E. Heggestad, R. J. Kohut, L. W. Kress, and P.J. Temple, Assessing impacts of ozone on agricultural crops, II, Crop yield functions and alternative exposure statistics, *JAPCA, 34*, 810-817, 1984.

Hoell, J. M., D. D. Davis, S. C. Liu, R. Newell, M. Shipham, H. Akimoto, R. J. McNeal, R. J. Bendura, and J. W. Drewry, Pacific Exploratory Mission-West A (PEM-West A): September-October 1991, *J. Geophys. Res., 101*, 1641-1653, 1996.

Hoell, J. M., D. D. Davis, S. C. Liu, R. E. Newell, H. Akimoto, R. J. McNeal, and R. J. Bendura, The Pacific Exploratory Mission-West Phase B (PEM-West B): February-March 1994, *J. Geophys. Res., 102*, 28,223-28,239, 1997.

Hogsett, W.E., J.E. Weber, D.T. Tingey, A.A. Herstrom, E.H. Lee, and J.A. Laurence, An approach for characterizing tropospheric ozone risk to forests, *Environ. Manage., 21*, 105-120, 1997.

Holton, J.R., On the global exchange of mass between the stratosphere and troposphere, *J. Atmos. Sci., 47*, 392-395, 1990.

Horowitz, L. W., and D. J. Jacob, Global impact of fossil fuel combustion on atmospheric NO_x, *J. Geophys. Res., 104*, 23,823-23,840, 1999.

Horowitz, L. W., J. Liang, G.M. Gardner, and D.J. Jacob, Export of reactive nitrogen from North America during summertime: Sensitivity to hydrocarbon chemistry, *J. Geophys. Res., 103*, 13,451-13,476, 1998.

Horvath, S.M., and D.J. McKee, Acute and chronic health effects of ozone, in Tropospheric Ozone: Human Health and Agricultural Impacts, edited by D. J. McKee, A.F. Lewis, New York, 1994.

Jacob, D. J., J. A. Logan, G. M. Gardner, R. M. Yevich, C. M. Spivakovsky, S. C. Wofsy, S. Sillman, and M. J. Prather, Factors regulating ozone over the United States and its export to the global atmosphere, *J. Geophys. Res., 98*, 14,817-14,826, 1993.

Jacob, D. J., et al., Origin of ozone and NO_x in the tropical troposphere: A photochemical analysis of aircraft observations over the South Atlantic basin, *J. Geophys. Res., 101*, 24,235-24,250, 1996.

Jacob, D.J., J.A. Logan, and P. P. Murti, Effect of rising Asian emissions on surface ozone in the United States, *Geophys. Res. Lett., 26*, 2175-2178, 1999.

Jaffe, D. A., R. E. Honrath, L. Zhang, H. Akimoto, A. Shimizu, H. Mukai, K. Murano, S. Hatakeyama, and J. Merrill, Measurements of NO, NO_y, CO, and ozone and estimation of the ozone production rate at Oki Island, Japan, during PEM-West, *J. Geophys. Res., 101*, 2037-2048, 1996.

Jaffe, D., A. Mahura, J. Kelly, J. Atkins, P. C. Novelli, and J. Merrill, Impact of Asian emissions on the remote North Pacific atmosphere: Interpretation of CO data from Shemya, Guam, Midway, and Mauna Loa, *J. Geophys. Res., 102*, 28,627-28,635, 1997.

Jaffe, D., et al., Transport of Asian air pollution to North America, *Geophys. Res. Lett,. 26*, 711-714, 1999.

Kajii, Y., K. Someno, H. Tanimoto, J. Hirokawa, H. Akimoto, T. Katsuno, and J. Kawara, Evidence for the seasonal variation of photochemical activity of tropospheric ozone: Continuous observation of ozone and CO at Happo, Japan, *Geophys. Res Lett., 25*, 3505-3508, 1998.

Kato, N., and H. Akimoto, Anthropogenic emissions of SO_2 and NO_x in Asia: Emission inventories, *Atmos. Environ.,Part A; 26*, 2997-3017, 1992.

Komala, N., S. Saraspriya, K. Kita, and T. Ogawa, Tropospheric ozone behavior observed in Indonesia, *Atmos. Environ., 30*, 1851-1856, 1996.

Lacis, A. A., D.J. Wuebbles, and J.A. Logan, Radiative forcing of climate by changes in the vertical distribution of ozone, *J. Geophys. Res., 95*, 9971-9981, 1990.

Lee, S.-H., H. Akimoto, H. Nakane, S. Kurnosenko, and Y. Kinjo, Lower tropospheric ozone trend observed in 1989-1997 at Okinawa, Japan, *Geophys. Res. Lett.*, 25, 1637-1640, 1998.

Liang, J., L. W. Horowitz, D. J. Jacob, Y. Wang, A. M. Fiore, J. L. Logan, G. M. Gardner, and J. W. Munger, Seasonal budgets of reactive nitrogen species and ozone over the United States, and export fluxes to the global atmosphere, *J. Geophys. Res., 103*, 13,435-13,450, 1998.

Lin, X., M. Trainer, and S. C. Liu, On the nonlinearity of the tropospheric ozone production, *J. Geophys. Res., 93*, 15,879-15,888, 1988.

Liu, S. C., D. Kley, M. McFarland, J D Mahlman, and H. Levy II, On the origin of tropospheric ozone, *J. Geophys. Res., 85*, 7546-7552, 1980.

Liu, S. C., M. Trainer, F. C. Fehsenfeld, D. D. Parrish, E. J. Williams, D. W. Fahey, G. Hubler, and P. C. Murphy, Ozone production in the rural troposphere and the implications for regional and global ozone distributions, *J. Geophys. Res., 92*, 4191-4207, 1987.

Liu, S.C., et al., Model study of tropospheric trace species distribution in PEM-West A, *J. Geophys. Res., 101*, 2073-2086, 1996.

Logan, J. A., Trends in the vertical distribution of ozone: An analysis of ozonesonde data, *J. Geophys. Res., 99*, 25,553-25,585, 1994.

Logan, J. A., M. J. Prather, S. C. Wofsy, and M. B. McElroy, Tropospheric chemistry: A global perspective, *J. Geophys. Res., 86*, 7210-7254, 1981.

Mauzerall, D. L., D. J. Jacob, S.-M. Fan, J. D. Bradshaw, G. L. Gregory, G. W. Sachse, and D. R. Blake, Origin of tropospheric ozone at remote high northern latitudes in summer, *J. Geophys. Res., 101*, 4175-4188, 1996.

Mauzerall, D. L., et al., Photochemistry in biomass burning plumes and implications for tropospheric ozone over the tropical South Atlantic, *J. Geophys. Res., 103*, 8401-8423, 1998.

Mauzerall, D.L., L.W. Horowitz, S. Walters, and G. Brasseur, A Comparison of the budgets and fluxes of tropospheric ozone over the United States, Europe, and East Asia using MOZART 2, a global photochemical model, *EoS Trans. AGU,80*(46), Fall Meet. Suppl., F234, 1999.

McKeen, S. A., E. -Y. Hsie, M. Trainer, R. Tallamraju, and S. C. Liu, A regional model study of the ozone budget in the eastern United States, *J. Geophys. Res., 96*, 10,809-10,845, 1991.

Merrill, J. T., M. Uematsu, and R. Bleck, Meteorological analysis of long-range transport of mineral aerosols over the North Pacific, *J. Geophys. Res., 94*, 8584-8598, 1989

Merrill, J. T., R. E. Newell, and A. S. Bachmeier, A meteorological overview for the Pacific Exploratory Mission-West Phase B, *J. Geophys. Res., 102*, 28,241-28,253, 1997.

Müller, J.-F., Geographical distribution and seasonal variation of surface emissions and deposition velocities of atmospheric trace gases, *J. Geophys. Res., 97*, 3787-3804, 1992.

Oltmans, S. J., et al., Trends of ozone in the troposphere, *Geophys. Res. Lett., 25*, 139-142, 1998.

Parrish, D. D., J. S. Holloway, M. Trainer, P. C. Murphy, G. L. Forbes, and F. C. Fehsenfeld, Export of North American ozone pollution to the North Atlantic Ocean, *Science, 259*,1436-1439, 1993.

Parrish, D. D., M. Trainer, J. S. Holloway, J. E. Yee, M. S. Warshawsky, F. C. Fehsenfeld, G. L. Forbes, and J. L. Moody, Relationships between ozone and carbon monoxide at surface sites in the North Atlantic region, *J. Geophys. Res., 103*, 13,357-13,376, 1998.

Penkett, S. A., N. J. Blake, P. Lightman, A. R. W. Marsh, P. Anwyl, and G. Butcher, The seasonal variation of nonmethane hydrocarbons in the free troposphere over the North Atlantic Ocean: Possible evidence for extensive reaction of hydrocarbons with the nitrate radical, *J. Geophys. Res., 98*, 2865-2885, 1993.

Pochanart, P., J. Hirokawa, Y. Kajii., H. Akimoto, and M. Nakao, Influence of regional-scale anthropogenic activity in northeast Asia on seasonal variations of surface ozone and its precursors observed at Oki, Japan, *J. Geophys. Res., 104*, 3621-3631, 1999.

Price, C., and D. Rind, A simple lightning parameterization for calculating global lightning distributions, *J. Geophys. Res., 97*, 9919-9933, 1992.

Rasch, P.J., and D. L. Williamson. Computational aspects of moisture transport in global models of the atmosphere, *Quart J. Roy. Meteorol. Soc., 116*, 1071-1090, 1990.

Rasch, P.J., N.M. Mahowald, and B. E. Eaton, Representations of transport, convection and the hydrologic cycle in chemical transport models: Implications for the modeling of short lived and soluble species, *J. Geophys. Res.. 102*, 28,127-28,138, 1997.

Thompson, A. M., The oxidizing capacity of the Earth's atmosphere: Probable past and future changes, *Science, 256*, 1157-1165, 1992.

Tsutsumi, M., Y. Igarashi, Y. Zaizen, and Y. Makino, Case studies of tropospheric ozone events observed at the summit of Mount Fuji, *J. Geophys. Res., 103*, 16,935-16,951, 1998.

van Aardenne, J. A., G. R. Carmichael, H. Levy II, D. Streets, and L. Hordjik, Anthropogenic NO_x emissions in Asia in the period 1990-2020, *Atmos. Environ., 33*, 633-646, 1999.

Williamson, D. L., and P. J. Rasch, Two-dimensional semi-Lagrangian transport with shape preserving interpolation, *Mon. Weather Rev., 117*, 102-129, 1989.

Yienger, J. J., A. A. Klonecki, H. Levy II, W. J. Moxim, and G. R. Carmichael, An evaluation of chemistry's role in winter-spring ozone maximum found in the northern midlatitude free troposphere, *J. Geophys. Res., 104*, 3655-3667, 1999.

H. Akimoto and D. Narita, Research Center for Advanced Science and Technology, University of Tokyo, Tokyo, 153-8904, Japan.

G. Brasseur, Max-Planck Institut für Meterologie, Bundersstraße 55 20416 Hamburg, Germany.

D.A. Hauglustaine, Service d'Aéronomie du CNRS, Université Paris 6, Tour 15-Aile 15-14, 4 Place Jussieu 75230, Paris, France.

L. Horowitz, Geophysical Fluid Dynamics Lab, P.O. Box 308, Princeton University, Princeton, NJ 08542-0308.

D.L. Mauzerall, Woodrow Wilson School of Public and International Affairs, Princeton University, Princeton, NJ 08540. (mauzerall@princeton.edu)

S. Walters, National Center for Atmospheric Research, P.O. Box 3000, Boulder, CO 80307-3000.

(Received October 7, 1999; revised January 27, 2000; accepted February 4, 2000.)